The Reactivity of Cyanogen towards Compounds containing Active Hydrogens at Carbon Atoms. Part 3.[1] Synthesis of Bis[1-cyano-2-(1-iminoethyl)butane-1,3-dionato]copper(II) from Cyanogen and Bis(acetylacetonato)copper(II): Kinetics, Thermodynamics and *X*-Ray Crystal Structure †

Benedetto Corain,* Marino Basato, and Giuseppina Visentin
Centro di Studio sulla Stabilita' e Reattivita' dei Composti di Coordinazione, C.N.R., Istituto di Chimica Analitica, 35100 Padova, Italy
Giuseppe Zanotti
Centro di Studio sui Biopolimeri, C.N.R., Istituto di Chimica Organica, 35100 Padova, Italy

---

The complex [Cu(acac)$_2$] (acac = acetylacetonate) reacts with C_2N_2 under ambient conditions in dichloroethane to give in high yield a compound of stoicheiometry [Cu(acacC_2N_2)$_2$]. An *X*-ray single-crystal analysis revealed that this is bis[1-cyano-2-(1-iminoethyl)butane-1,3-dionato]copper(II), apparently derived from bis[3-(cyanoiminomethyl)pentane-2,4-dionato]copper(II) formed upon insertion of C_2N_2 into the methine C–H bonds in [Cu(acac)$_2$]. The kinetics of the cyanation process reveal that it occurs in two distinct steps, which display similar second-order rate constants. The kinetic and thermodynamic role of the complex [Cu(acac)$_2$] is discussed.

The reaction of cyanogen with β-dicarbonyl compounds in ethanol is a base-catalysed process, known since 1898.[2] The reaction (i) can be envisaged as an insertion of the C_2N_2 moiety into the methine C–H bond of the organic substrate enolic form.

This process may be of some synthetic interest in that it doubles the degree of functionalization of the organic reagent by introducing the two groups C=NH and C≡N.

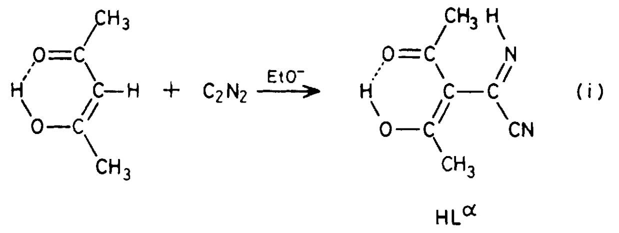

(i)

We have recently found [1a] that this cyanoiminomethylation reaction can occur also at a metal-co-ordinated pentane-2,4-dionate ligand (acac$^-$) (metal = Mn^{II}, Mn^{III}, Fe^{II}, Co^{II}, Ni^{II}, or Cu^{II}), though the reaction is strongly dependent on the metal (it fails for Cr^{III} and Pd^{II}) and gives analytically pure [M(acacC_2N_2)$_2$] only in the case of [Ni(acac)$_2$] and [Cu(acac)$_2$].

In view of the fact that this reaction of cyanogen is a novelty in its co-ordination chemistry [1b] and also because those acetylacetonate complexes found to be reactive with cyanogen [1] catalyse not only the cyanation reaction mentioned above but also the subsequent dimerization of the primary organic product to a heavily functionalized pyrimidine [1a] (L) (Scheme 1), we have studied in detail the mechanism of the reaction of [Cu(acac)$_2$] with C_2N_2 and the thermodynamics of the [Cu(acac)$_2$]/HL$^{\alpha}$ and [Cu(acacC_2N_2)$_2$]/Hacac exchanges, which have been shown to be key steps in the copper-catalysed pyrimidine synthesis.[1a,3] Furthermore the addition–insertion product [Cu(acacC_2N_2)$_2$] has been fully characterized by *X*-ray analysis and other physical properties. For this copper(II) complex a structure identical with that of [NiL$^{\alpha}_2$] was proposed [1b] as the result of the similarity of the Debye spectra of the two species.

The complex [NiL$^{\alpha}_2$] is the primary product of the reaction of [Ni(acac)$_2$] with C_2N_2; upon recrystallization at 60 °C it changes into the more stable bis[1-cyano-2-(1-iminoethyl)-butane-1,3-dionato]nickel(II) complex (hereafter referred to as [NiL$^{\beta}_2$]), for which the *X*-ray single-crystal structure was determined. However, whether [NiL$^{\alpha}_2$] is a real isomer or a dimorphic form of [NiL$^{\beta}_2$] is still not unambiguously established.[1b]

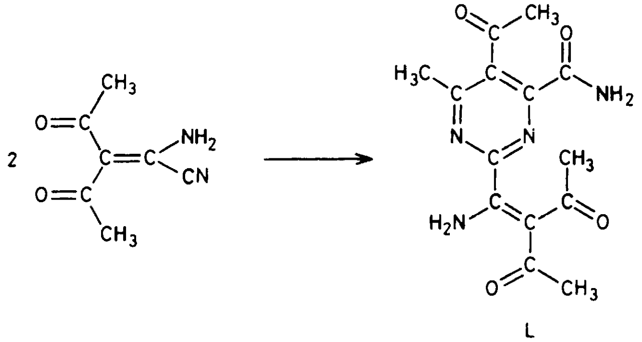

Scheme 1.

Experimental

Solvents were purified and dried by standard procedures. In particular, CH_2Cl_2 (Baker Bar) was treated with aqueous sodium carbonate, dried over sodium sulphate, and then distilled. Cyanogen was a Union Carbide reagent and was used as received. The preparation of stock solutions of C_2N_2 and the determination of their concentrations were carried out as described previously.[4]

Details for the preparation of [CuL$^{\beta}_2$] can be found elsewhere.[1] Crystals suitable for *X*-ray analysis were obtained from a solution prepared from [Cu(acac)$_2$] (100 mg) in CH_2Cl_2 (6 cm^3) containing C_2N_2 (0.25 mol dm^{-3}). The solution gave dark green crystals (94 mg) after 24 h at *ca.* 20 °C.

Routine i.r. spectra were recorded on a Perkin-Elmer 257 instrument; accurate ones on a 599 B model. Electronic spectra were recorded on a Perkin-Elmer A 72 spectrophotometer.

---

† *Supplementary data available* (No. SUP 23551, 9 pp.): observed and calculated structure factors, positional and thermal parameters. See Notices to Authors No. 7, *J. Chem. Soc., Dalton Trans.*, 1981, Index issue.

X-*Ray Structure Analysis of* [CuL$^{\beta}{}_2$].—*Crystal data* (*from single-crystal diffractometry*). $C_{14}H_{14}CuN_4O_4$, M = 365.0, a = 11.460(7), b = 6.112(5), c = 5.611(4) Å, α = 79.5(1), β = 91.5(1), γ = 104.0(1)°, U = 375.0 Å^3, Z = 1, D_c = 1.62 g cm^{-3}, F(000) = 187.0, λ(Mo-K_α) = 0.7107 Å, μ(Mo-K_α) = 1.54 cm^{-1}, space group $P\bar{1}$.

The intensities were collected on a Philips PW1100 four-circle diffractometer operating in the $\theta/2\theta$ scan mode (scan width 1.0°, scan speed 0.002° s^{-1}); 1 320 independent reflections up to $\theta = 25°$ were measured, of which 1 097 had intensities greater than 2.5 times their standard deviation (σ, calculated from the counting statistics of the measurements). During data collection, two standard reflections were measured every 180 min to check the stability of the crystal and the electronics. The intensities were corrected for Lorentz and polarization factors, and an experimental absorption correction was applied following the method proposed by North *et al.*[5] A Fourier map was calculated by putting the copper atom at the origin, and the rest of the molecule was immediately evident. The structure was refined by the full-matrix least-squares method, allowing the Cu, O, and N atoms to vibrate anisotropically. The H atoms of the methyl groups were constrained to their normal geometry by using the group refinement procedure.[6] The H atom bound to the imine nitrogen was not localized in the Fourier difference map.

Throughout the analysis the scattering factors of ref. 7 were used; both real and imaginary parts of the anomalous dispersion were included for copper only.

The final R factor was 0.062 (R' = 0.066). The last cycles of refinement were carried out by minimizing the quantity $\Sigma_w[(F_o)^2 - (F_c)^2]$, $w = 3.52/[\sigma^2(F) + 0.01\,(F)^2]$.

All the calculations were carried out on the IBM 370/158 computer of the University of Padova, with the SHELX 76 [8] system of programs.

Experimental Kinetic Procedures and Mathematical Treatment.—Thermodynamics of the [Cu(acac)$_2$]/[CuL$^{\beta}{}_2$] *system.* Solutions of [Cu(acac)$_2$] and of [CuL$^{\beta}{}_2$] were found to obey the Beer–Lambert law in the concentration range employed. The coproportionation equilibrium constants were determined by two different procedures.

(*a*) The solutions of [Cu(acac)$_2$] and [CuL$^{\beta}{}_2$] were placed in the two halves of a tandem cell and their total absorbance was balanced with a convenient reference. After mixing of the reaction solutions (in the tandem cell), the spectrum of the mixture gave directly ΔA values at various wavelengths ($\Delta A = A_{eq} - A_0$). The absorbances at and before equilibration are defined as in equations (1) and (2), where ε_A refers to [Cu(acac)$_2$], ε_B to [CuL$^{\beta}{}_2$], and ε_{AB} to [Cu(acac)L$^{\beta}$].

$$A_0 = \varepsilon_A\{2[\mathrm{Cu(acac)_2}]_0\}l/2 + \varepsilon_B(2[\mathrm{CuL^{\beta}{}_2}]_0)l/2 \qquad (1)$$

$$A_{eq} = \varepsilon_A\{[\mathrm{Cu(acac)_2}]_0 - x\}l + \varepsilon_B([\mathrm{CuL^{\beta}{}_2}]_0 - x)l + \varepsilon_{AB}2xl \qquad (2)$$

Here 2[Cu(acac)$_2$]$_0$ and 2[CuL$^{\beta}{}_2$]$_0$ are the concentrations of the solutions in the two halves of the cells; [Cu(acac)$_2$]$_0$ and [CuL$^{\beta}{}_2$]$_0$ are the initial concentrations after mixing; $2x$ is the concentration of [Cu(acac)L$^{\beta}$] at equilibrium; and l is the cell pathlength.

(*b*) The measurements were performed with 0.1 cm cells containing, separately, [Cu(acac)$_2$], [CuL$^{\beta}{}_2$], and the mixture obtained by mixing equal volumes of these two solutions.

The two experimental methods gave consistent ΔA values, from which the equilibrium concentrations and the related equilibrium constant could be obtained as indicated in the Discussion section.

Reaction of 3-(*Cyanoiminomethyl*)*pentane*-2,4-*dione* (HL$^{\alpha}$) *with* [Cu(acac)$_2$].—In order to calculate values for the equilibrium constants of reactions (8) and (9) (see later) we employed a fitting method, *i.e.* we determined the concentration values of the various species involved which minimized the differences between calculated and observed spectra of the mixture. Equation (3) was used, where x = concentration of [Cu(acac)L$^{\beta}$] at equilibrium, y = concentration of [CuL$^{\beta}{}_2$] at equilibrium, C = initial concentration of [Cu(acac)$_2$], and C_1 = initial concentration of HL$^{\alpha}$.

$$A_{eq}/l = \varepsilon_A(C - x - y) + \varepsilon_{HL^{\alpha}}(C_1 - x - 2y) + \varepsilon_{AB}x + \varepsilon_{Hacac}(x + 2y) + \varepsilon_B y \qquad (3)$$

This fitting was applied at six different wavelengths (270—320 nm) characterized by large absorbance changes during the reaction.

Kinetics of Cyanation of [Cu(acac)$_2$].—The method employed to determine the reaction profiles can be summarized as follows.

(*a*) Three particular λ values were chosen: 305, 270, and 340 nm. At 305 nm $\varepsilon_A = \varepsilon_{AB}$, whereas at 270 and 340 nm large absorbance changes are observed upon reaction.

(*b*) From the absorbance values, at various times, at the three chosen wavelength values, the actual concentration of each species was determined according to equation (4), where

$$A/l = \varepsilon_A(C - x - y) + \varepsilon_{AB}x + \varepsilon_B y \qquad (4)$$

C = initial concentration of [Cu(acac)$_2$], x = concentration at a given time of [Cu(acac)L$^{\beta}$], y = concentration at a given time of [CuL$^{\beta}{}_2$], and l = cell pathlength.

At 305 nm equation (4) reduces to $A/l = A_0/l + y(\varepsilon_B - \varepsilon_A)$, which makes possible direct determination of y. The uncertainty in y is indeterminate, whereas for [Cu(acac)$_2$] and [Cu(acac)L$^{\beta}$] it may be represented by the differences between the values of the concentrations calculated at 270 and 340 nm.

Results and Discussion

Synthesis and Characterization of the Complex [Cu(acacC$_2$N$_2$)$_2$].—The i.r. spectrum of the methylene chloride solution under preparative conditions {[Cu(acac)$_2$] = 0.08 mol dm^{-3}; [C$_2$N$_2$] = 0.25 mol dm^{-3}} displays the same two bands (at 3 330 and 1 665 cm^{-1}) as a solution obtained by dissolving an authentic sample of [Cu(acacC$_2$N$_2$)$_2$]. The solid compound displays i.r. bands at 3 270 (ν_{N-H}), 2 225 ($\nu_{C\equiv N}$), 1 635 ($\nu_{C=N}$), and 1 555 cm^{-1} ($\nu_{C=O}$).

The u.v.-visible spectra of the product in CH$_2$Cl$_2$ solution and in the solid state (Nujol mull) are practically identical, indicating identical or very similar molecular structures in both phases.* The product exhibits poor thermal stability: thermogravimetric analysis shows that it is stable in the narrow temperature range 160—170 °C, under argon, beyond which thermal decomposition occurs. Mass measurements carried out in the thermal stability temperature range give clean spectra with a strong parent-ion peak (Found: M, 365.0. Calc. M, 365.0). The magnetic moment, measured by the Gouy method on solid samples, is 2.03 B.M. (1.88 × 10^{-23} J T^{-1}) On the basis of these data and of analogy with a closely related Ni^{II} compound,[1b] two possible molecular structures [(1)

---

* The spectral data reported for this compound in ref. 1*a* refer erroneously to the related Ni^{II} species described in Part 1 (ref. 1*b*). The correct figures are [λ/nm (ε/dm^3 mol^{-1} cm^{-1})]: 270 (16 900), 287 (17 900), and 344 (12 400).

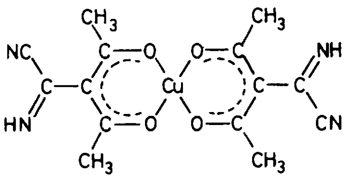

(1) $[CuL^{\alpha}_2]$

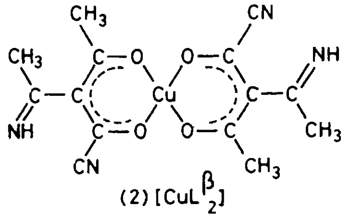

(2) $[CuL^{\beta}_2]$

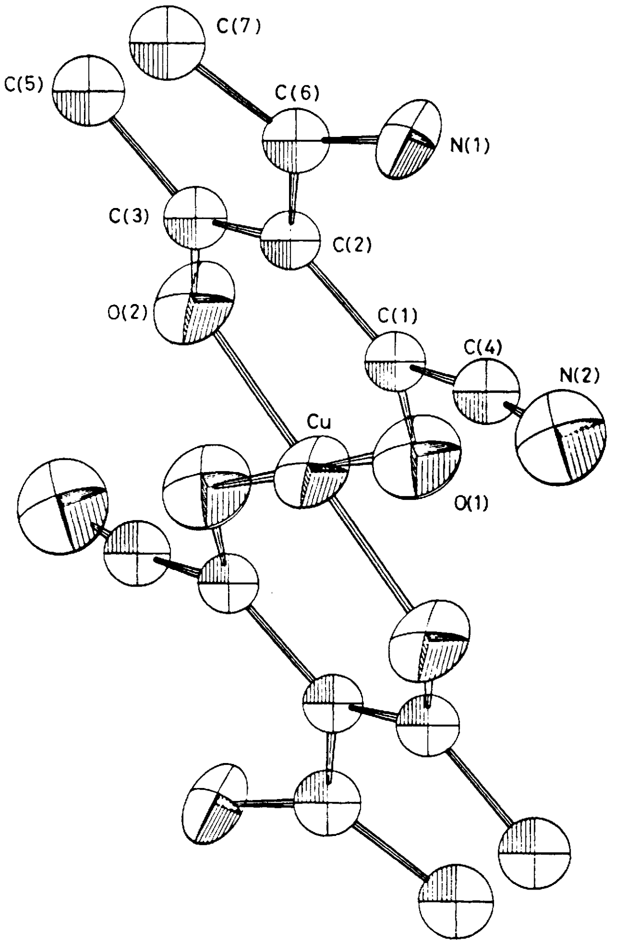

Figure 1. Single-crystal *X*-ray structure of $[CuL^{\beta}_2]$, with the atomic numbering system used (hydrogen atoms not shown)

Table 1. Final positional parameters (with e.s.d.s in parentheses) for non-H atoms in $[CuL^{\beta}_2]$

Atom	*X*/*a*	*Y*/*b*	*Y*/*c*
Cu	0.0	0.0	1.0
O(1)	0.0466(5)	0.2508(9)	1.1696(9)
O(2)	0.1459(4)	0.1093(8)	0.8113(9)
N(1)	0.3594(5)	0.7239(9)	1.1569(9)
N(2)	0.1246(6)	0.7107(9)	1.4008(12)
C(1)	0.1437(5)	0.4165(10)	1.1345(11)
C(2)	0.2405(5)	0.4420(10)	0.9664(10)
C(3)	0.2348(5)	0.2776(10)	0.8138(10)
C(4)	0.1447(6)	0.5925(11)	1.2814(11)
C(5)	0.3340(6)	0.2797(12)	0.6422(13)
C(6)	0.3447(6)	0.6369(11)	0.9758(11)
C(7)	0.4331(6)	0.7420(13)	0.7688(13)

Table 2. Bond lengths (Å) and angles (°) in $[CuL^{\beta}_2]$

Cu–O(1)	1.910(4)	C(1)–C(4)	1.467(7)
Cu–O(2)	1.913(4)	C(3)–C(5)	1.505(8)
O(1)–C(1)	1.303(6)	C(2)–C(6)	1.477(7)
O(2)–C(3)	1.263(6)	C(6)–C(7)	1.504(8)
C(1)–C(2)	1.436(7)	C(4)–N(2)	1.135(7)
C(2)–C(3)	1.423(7)	C(6)–N(1)	1.220(7)
O(1)–Cu–O(2)	90.0(2)	C(1)–C(4)–N(2)	168.0(6)
Cu–O(1)–C(1)	127.7(4)	C(1)–C(2)–C(6)	115.7(5)
Cu–O(2)–C(3)	132.3(4)	C(3)–C(2)–C(6)	124.2(5)
O(1)–C(1)–C(2)	126.6(5)	C(5)–C(3)–C(2)	112.1(5)
C(1)–C(2)–C(3)	120.0(5)	C(2)–C(6)–C(7)	123.5(5)
C(2)–C(3)–O(2)	123.4(5)	C(2)–C(6)–N(1)	119.2(5)
O(1)–C(1)–C(4)	112.9(5)	C(7)–C(6)–N(1)	117.2(5)
C(2)–C(1)–C(4)	120.5(5)		

Table 3. Some least-squares planes [a] in the complex $[CuL^{\beta}_2]$, with torsion angle and deviations (Å) of atoms from the respective planes

Plane A: $0.455x - 0.679y + 0.576z = 3.232$

Cu	0.0	C(1)*	0.030
O(1)	0.0	C(2)*	−0.004
O(2)	0.0	C(3)*	−0.028
		C(6)*	0.060

Plane B: $0.580x - 0.775y + 0.252z = 1.524$

N(1)	0.0	C(2)*	−0.047
C(6)	0.0	C(7)	0.0

Torsion angle between planes A and B: 20.8°.

[a] The equations of the planes are in the form $Ax + By + Cz = D$, in orthogonal Å space with x parallel to a^*, y parallel to $c \times a^*$, and z parallel to c. An asterisk denotes an atom not used in the plane calculation.

and (2)] appear conceivable. An *X*-ray single-crystal analysis confirmed structure (2), $[CuL^{\beta}_2]$.

The molecular structure of $[CuL^{\beta}_2]$ is shown in Figure 1. The final structural parameters for non-hydrogen atoms are reported in Table 1, and bond lengths and angles in Table 2.

The molecule exhibits marked similarities to $[NiL^{\beta}_2]$,[1b] despite some significant differences. It possesses a centre of symmetry; the copper atom shows an exact square-planar co-ordination geometry, the O–Cu–O angles being 90.0°, with the four oxygen atoms exactly in the same plane. The two Cu–O distances are very similar, despite the inductive effect of the C≡N group, and are in good agreement with the values in other square-planar complexes of Cu^{II} [1.90—1.91(1) Å in bis(3-phenylpentane-2,4-dionato)copper(II)[9] and 1.89—1.92(1) Å in bis(ethyl acetoacetato)copper(II)[10]].

Bond distances and angles for the rest of the molecule are similar, within experimental error, to those in $[NiL^{\beta}_2]$. However, significant differences can be seen in the conformations of the two molecules; in $[CuL^{\beta}_2]$ the CuOCCCO ring is nearly planar (Table 3), while in $[NiL^{\beta}_2]$ the OCCCO plane is tilted by 52.6(1)° with respect to the ONiO plane. This fact, along

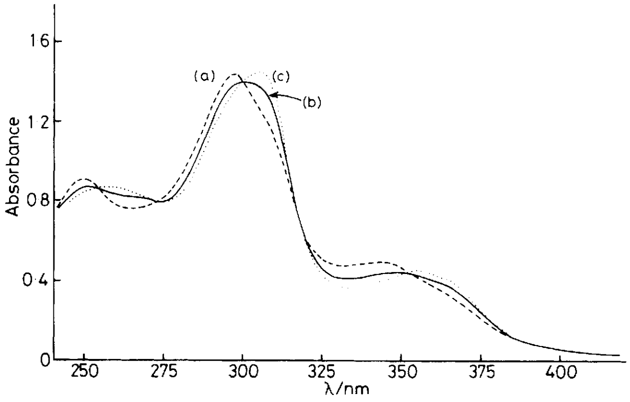

Figure 2. Comparison of (a) the combined spectra of $[\mathrm{Cu(acac)_2}]$ and $[\mathrm{CuL^{\beta}_2}]$ with (b) that of a solution obtained upon mixing equimolar solutions of these reagents and with (c) the calculated spectrum for quantitative conversion into $[\mathrm{Cu(acac)L^{\beta}}]$ $\{[\mathrm{Cu(acac)_2}]_0 = [\mathrm{CuL^{\beta}_2}]_0 = 4.03 \times 10^{-5}$ mol dm^{-3}, cell pathlength 0.439 cm × 2, reference $\mathrm{CH_2Cl_2}\}$

Table 4. Optical density changes at 368 nm as a function of the relative concentrations of $[\mathrm{Cu(acac)_2}]$ and $[\mathrm{CuL^{\beta}_2}]$

$[\mathrm{CuL^{\beta}_2}]_0$ / mol dm^{-3}	$[\mathrm{Cu(acac)_2}]_0$ / mol dm^{-3}	ΔA_{exp}	ΔA_{norm} [c]
2.51×10^{-5}	1.01×10^{-4}	0.040 [a]	0.045
	2.01×10^{-4}	0.044 [a]	0.050
	5.03×10^{-4}	0.046 [a]	0.052
	1.00×10^{-3}	0.047 [a]	0.053
	2.01×10^{-3}	0.046 [a]	0.052
	5.03×10^{-3}	0.046 [a]	0.052
1.03×10^{-4}	5.10×10^{-5}	0.074 [a]	0.08
	1.02×10^{-4}	0.118 [a]	0.13
	2.04×10^{-4}	0.150 [a]	0.17
	5.11×10^{-4}	0.172 [a]	0.19
	1.02×10^{-3}	0.178 [a]	0.20
2.01×10^{-4}	1.98×10^{-5}	0.002 [b]	0.02
	4.94×10^{-5}	0.009 [b]	0.09
	1.98×10^{-4}	0.022 [b]	0.22
	4.94×10^{-4}	0.033 [b]	0.33
	9.89×10^{-4}	0.034 [b]	0.34
	1.98×10^{-3}	0.040 [b]	0.40
	4.94×10^{-3}	0.041 [b]	0.41
4.95×10^{-4}	2.48×10^{-4}	0.043 [b]	0.43
	4.97×10^{-4}	0.065 [b]	0.65
	9.94×10^{-4}	0.089 [b]	0.89
	2.48×10^{-3}	0.103 [b]	1.03
	4.97×10^{-3}	0.102 [b]	1.02

[a] Cell pathlength 0.439 cm × 2. [b] Cell pathlength 0.1 cm. [c] Values normalised to 1 cm pathlength.

with the C(2)–C(6) torsion angle of 21°, suggests that some resonance could extend from the imino group to the 1,3-diketonate moiety. This is in agreement with the higher symmetry of the bond distances in $[\mathrm{CuL^{\beta}_2}]$ (as compared with $[\mathrm{NiL^{\beta}_2}]$), despite the small difference between C(1)–O(1) and C(3)–O(2), which can be explained by the different substituents on C(1) and C(3) atoms.

The slightly different conformations of $[\mathrm{CuL^{\beta}_2}]$ and $[\mathrm{NiL^{\beta}_2}]$ could also explain the different crystal packing of the two compounds, despite the similar molecular geometry.

The observed structure of $[\mathrm{CuL^{\beta}_2}]$ contradicts the previous attribution for the same compound,[1a] which was based on the close similarity of its Debye spectrum to that of $[\mathrm{NiL^{\alpha}_2}]$.[1b] These results cast doubt on the proposed structure of $[\mathrm{NiL^{\alpha}_2}]$, and further investigations are required.

Thermodynamics and Kinetics of the System $[\mathrm{Cu(acac)_2}]/\mathrm{C_2N_2}$.—*Ligand coproportionation reaction.* In a preliminary experiment it was shown that equimolar solutions of $[\mathrm{Cu(acac)_2}]$ and $[\mathrm{CuL^{\beta}_2}]$ (403×10^{-5} mol dm^{-3}) react rapidly (t_∞ *ca.* 10 min) to give an equilibrium mixture with a u.v.–visible spectrum appreciably different from the sum of the spectra of the reagents (see Experimental section for details). This indicated the formation of a new species, considered to be closely related to $[\mathrm{Cu(acac)_2}]$ and $[\mathrm{CuL^{\beta}_2}]$ (Figure 2).

Literature data for similar situations relevant to β-diketonate[11] complexes show that under these conditions coproportionation reactions take place to give mixed complexes, *i.e.* metal[β-diketonate (A)][β-diketonate (B)]. This means that, in our case, reaction (5) apparently occurs.

$$[\mathrm{Cu(acac)_2}] + [\mathrm{CuL^{\beta}_2}] \overset{K}{\rightleftharpoons} 2[\mathrm{Cu(acac)L^{\beta}}] \qquad (5)$$

Attempts to isolate $[\mathrm{Cu(acac)L^{\beta}}]$ in reasonably pure form were unsuccessful, but its existence could be inferred from a careful spectrophotometric study of reaction (5) at various values of $[\mathrm{Cu(acac)_2}]/[\mathrm{CuL^{\beta}_2}]$.

Table 4 reports the concentrations of the reacting complexes together with the relevant ΔA values obtained at 368 nm (details of the methods are in the Experimental section).

In our treatment, ΔA is the difference between the absorbance of the mixture at (A_{eq}) and before (A_0) equilibration [equation (6)]. This quantity is a function of the difference in molar absorption coefficients of the product and the reagents, of x {the concentration of 'reacted' $[\mathrm{Cu(acac)_2}]$ and $[\mathrm{CuL^{\beta}_2}]$},

$$\Delta A = A_{\mathrm{eq}} - A_0 = \varepsilon x l \qquad (6)$$

$$\varepsilon = 2\varepsilon_{\mathrm{AB}} - \varepsilon_{\mathrm{A}} - \varepsilon_{\mathrm{B}} \qquad (7)$$

and of l (the cell pathlength); $\varepsilon_{\mathrm{AB}}$ refers to $[\mathrm{Cu(acac)L^{\beta}}]$}, ε_{A} to $[\mathrm{Cu(acac)_2}]$, and ε_{B} to $[\mathrm{CuL^{\beta}_2}]$.

The data in Table 4 show that for each series of reactions the ΔA figures increase with increasing initial $[\mathrm{Cu(acac)_2}]$ concentration to reach a limiting value (ΔA_{lim}) corresponding to complete conversion of the reagent present at lower concentration ($[\mathrm{CuL^{\beta}_2}]$ in our case) into the mixed species. From these values it is possible to calculate ε from the relation $\varepsilon = \Delta A_{\mathrm{lim}}/(l[\mathrm{CuL^{\beta}_2}]_0)$ and, as a consequence, from known values of ε_{A} and ε_{B}, the molar absorption coefficient of $[\mathrm{Cu(acac)L^{\beta}}]$.

In this respect it is noteworthy that the $\varepsilon_{\mathrm{AB}}$ values determined at various values of $[\mathrm{CuL^{\beta}_2}]_0$ and by different experimental methods (see Experimental section) are consistent with an average figure of 2 042 ± 74, suggesting the formation of a single compound, *i.e.* $[\mathrm{Cu(acac)L^{\beta}}]$.

At this point, the ε value obtained, inserted in equation (6) allows one to calculate x and K for the coproportionation reaction (5), $K = (2x)^2/\{([\mathrm{Cu(acac)_2}]_0 - x)([\mathrm{CuL^{\beta}_2}]_0 - x)\}$. To determine the K value for each set of data, only ΔA values in the range $(0.2\text{—}0.8)\Delta A_{\mathrm{lim}}$ were considered; out of this range the error in x becomes too high.

Again, the consistency of the obtained K values (average 10 ± 3) supports the validity of the stoicheiometry indicated [reaction (5)]. A further step in this treatment, relevant to the following ligand exchange and cyanation studies, involves the calculation of the u.v.–visible spectrum of $[\mathrm{Cu(acac)L^{\beta}}]$ in the range 240—420 nm. In fact, from Figure 2 and by using

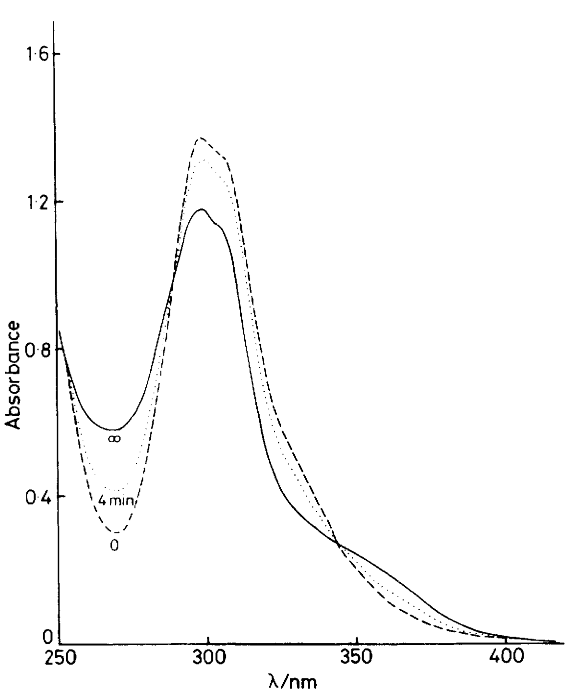

Figure 3. Typical spectral changes observed upon addition of HL^α to solutions of $[Cu(acac)_2]$

the equation (6), one can calculate x from the experimental ΔA value at 368 nm and then, by introducing the resulting x value, obtain the ε values at other wavelengths from the experimental ΔA values.

Figure 2 also shows the calculated spectrum of $[Cu(acac)L^\beta]$ at a concentration twice that of $[Cu(acac)_2]$ and $[CuL^\beta_2]$. As expected [12] this spectrum does not differ markedly from the sum of the $[Cu(acac)_2]$ and $[CuL^\beta_2]$ spectra, although a shift of 10 nm of the maximum around 300 nm is observed.

Ligand exchange (*with protonation*) *reactions.* $[Cu(acac)_2]$ reacts with HL^α according to equations (8) and (9). Figure 3 shows the typical spectral behaviour observed in the range 250—420 nm for these substitution reactions, which are fast ($t_{\frac{1}{2}}$ *ca.* 5 min). Two runs were performed with $[Cu(acac)_2]_0 = 5.1 \times 10^{-5}$ mol dm^{-3} and 1 : 1 and 1 : 4 $[Cu^{II}] : HL^\alpha$ ratios. In both experiments and at all six investigated wavelengths (see Experimental section) the difference between calculated and observed absorbance figures was less than 4%. The procedure employed led to values of $K_1 = 0.83 \pm 0.01$, $K_2 = 0.10 \pm 0.02$, $K_{1,2} = K_1K_2 = 0.08 \pm 0.02$, and to a value of 8 ± 2 for the coproportionation reaction constant. The excellent fitting obtained for the system described by equations (8) and (9) is a strong indication that the mixed complex is $[Cu(acac)L^\beta]$ and not $[Cu(acac)L^\alpha]$, even though the spectra of these species may not be very different.[12] This implies that the expected [13] preliminary direct formation of $[Cu(acac)L^\alpha]$ is followed by fast isomerization to $[Cu(acac)L^\beta]$. A mechanism for this isomerization has been proposed already in the nickel(II) case.[1b]

$$[Cu(acac)_2] + HL^\alpha \overset{K_1}{\rightleftharpoons} [Cu(acac)L^\beta] + Hacac \quad (8)$$

$$[Cu(acac)L^\beta] + HL^\alpha \overset{K_2}{\rightleftharpoons} [CuL^\beta_2] + Hacac \quad (9)$$

We have also investigated the $[Cu(acac)_2]/HL^\alpha/[CuL^\beta_2]/$Hacac system, starting from $[CuL^\beta_2]$ and Hacac. Spectrophotometric studies (u.v.–visible) show clearly that $[CuL^\beta_2]$ reacts rapidly (t_∞ *ca.* 30 min) with Hacac, but no spectral fitting was obtained in agreement with the reverse of equations (8) and (9) ($[Cu^{II}] = 5.2 \times 10^{-5}$ mol dm^{-3}; [Hacac] = 1—20 $\times 10^{-5}$ mol dm^{-3}). Then we studied the reaction between $[CuL^\beta_2]$ and Hacac under preparative conditions, following it by i.r. spectroscopy. Analysis of the solution after addition of Hacac revealed that a species related to HL^α (ν_{N-H} 3 460 cm^{-1}) is immediately liberated from $[CuL^\beta_2]$, and i.r. analysis of the solid residue left after evaporation indicated that HL^α, L (see Scheme 1), and $[Cu(acac)_2]$ (in similar proportions) are the products of this evidently very complex reaction.

These i.r. and preparative data suggest that the interaction of Hacac with $[CuL^\beta_2]$ cannot be seen simply as giving rise to the reverse of equations (8) and (9), but as a more complex reacting system.

Cyanation of $[Cu(acac)_2]$: *preparative and kinetic aspects.* When solutions of $[Cu(acac)_2]$ (5×10^{-3} mol dm^{-3}) are made 0.6 mol dm^{-3} in C_2N_2, the initial blue colour turns gradually to green and a medium-strong i.r. band develops at 3 330 cm^{-1}. After about 24 h at room temperature, $[CuL^\beta_2]$ begins to separate in high yield.[1a]

When a blue suspension of $[Cu(acac)_2]$ in CH_2Cl_2 (2.0 mmol in 20 cm^3) is made 0.86 mol dm^{-3} in C_2N_2 and stirred vigorously, the i.r. spectrum of the supernatant solution (0.1 mm cell) displays a clear parallel development of two bands at 1 525 and 1 560 cm^{-1}. These bands are seen also in solutions of $[Cu(acac)_2]$ and $[CuL^\beta_2]$ respectively; however that at 1 525 cm^{-1} cannot be due to $[Cu(acac)_2]$ {its concentration is 'buffered' by undissolved $[Cu(acac)_2]$ for 40 min at *ca.* 20 °C}. The colour of the suspension turns gradually to green and the intensity of the 1 525 and 1 560 cm^{-1} bands begins to decrease after *ca.* 45 min.

These two observations indicate that under homogeneous phase conditions at $[Cu^{II}] = 5 \times 10^{-3}$ mol dm^{-3} species containing a $>C=N-H$ group develop gradually. Under heterogeneous phase conditions, however, the data are more revealing and strongly suggest that a species containing both $acac^-$ and $acac{\cdot}C_2N_2^-$ co-ordinated to Cu^{II} forms in solution. This complex is presumably the mixed $[Cu(acac)L^\beta]$ species, which we have clearly deduced from the equilibration experiments discussed above and by the following kinetic evidence.

Kinetics of the Cyanation of $[Cu(acac)_2]$.—The overall stoicheiometric process (10) occurs in two well separated consecutive steps, (11) and (12). This system is complicated by the occurrence of the coproportionation reaction (5), which is fast (t_∞ *ca.* 20 min) compared with processes (11) and (12). A typical spectral change observed upon reaction of C_2N_2 with $[Cu(acac)_2]$ is shown in Figure 4.

$$[Cu(acac)_2] + 2C_2N_2 \longrightarrow [CuL^\beta_2] \quad (10)$$

$$[Cu(acac)_2] + C_2N_2 \xrightarrow{k_1} [Cu(acac)L^\beta] \quad (11)$$

$$[Cu(acac)L^\beta] + C_2N_2 \xrightarrow{k_2} [CuL^\beta_2] \quad (12)$$

It was found most convenient to calculate k_1 and k_2 by previous determination of the concentration *vs.* time profiles of $[Cu(acac)_2]$, $[Cu(acac)L^\beta]$, and $[CuL^\beta_2]$ (Figure 5). The actual concentration of each species could be obtained by measuring the absorbances at various times at three wavelengths {and by knowing that $[Cu(acac)_2] + [Cu(acac)L^\beta] + [CuL^\beta]_2 = [Cu(acac)_2]_0$}.

The behaviour shown in this and similar studies under different conditions is qualitatively consistent with the proposed cyanation sequence and with the coexisting ligand co-

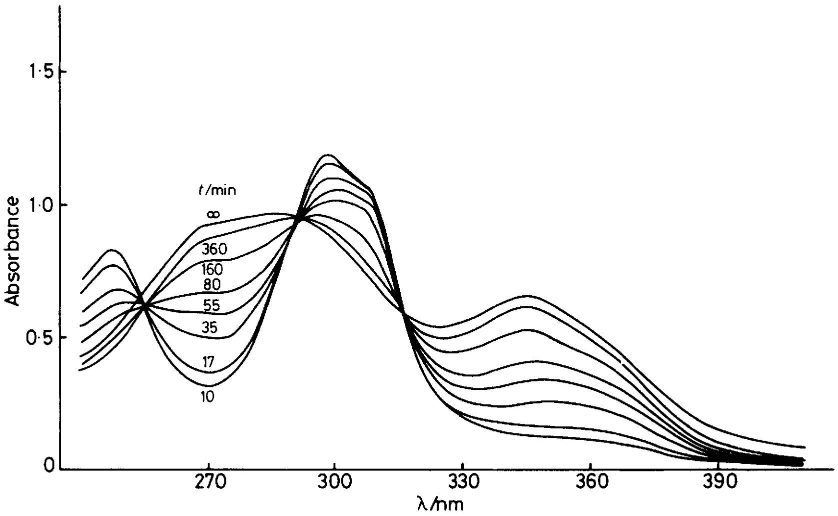

Figure 4. Spectral changes upon cyanation of [Cu(acac)$_2$] by C_2N_2 ([Cu^{II}] = 5.0 × 10^{-3} mol dm^{-3}; [C_2N_2] = 0.53 mol dm^{-3}; cell pathlength 0.01 cm)

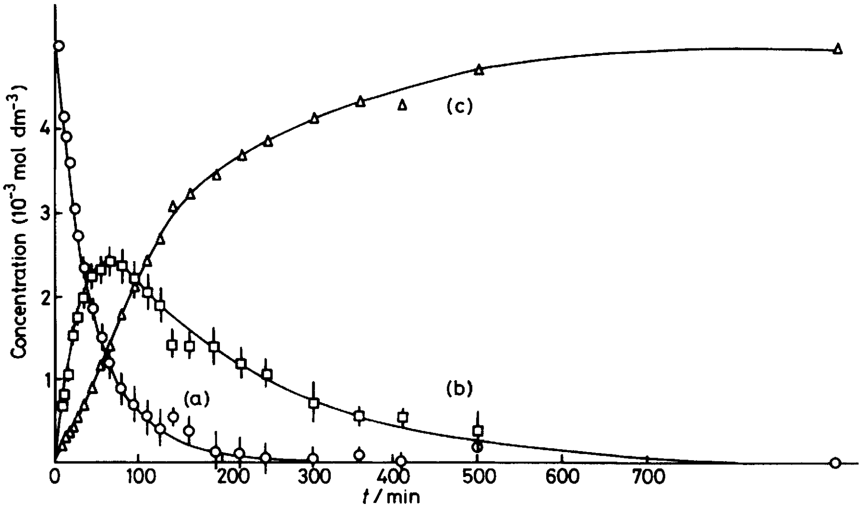

Figure 5. Concentration *vs.* time profiles of (a) [Cu(acac)$_2$], (b) [Cu(acac)L$^\beta$], and (c) [CuL$^\beta_2$] at [C_2N_2] = 0.53 mol dm^{-3}, [Cu^{II}] = 5.0 × 10^{-} mol dm^{-3}

proportionation equilibrium. In particular the relatively short induction period observed for [CuL$^\beta_2$] is in agreement with the circumstance that [CuL$^\beta_2$] is formed not only by cyanation of [Cu(acac)L$^\beta$], but also by fast ligand disproportionation reactions of the mixed complex. Quantitative kinetic information could be obtained from this type of study by working with a suitable excess of C_2N_2 over Cu^{II} and in selected time ranges where the kinetic rate law takes a simplified form. A logarithmic plot of [Cu(acac)$_2$] concentration *vs.* time (conditions of Figure 5) exhibits a fairly good linear behaviour for almost twice $t_{\frac{1}{2}}$, thus furnishing the $k_{obs.}$ figure for the first cyanation process {the same behaviour was observed with ten times lower initial [Cu(acac)$_2$] = 5 × 10^{-4} mol dm^{-3}}.

The $k_{obs.}$ value for the second step was obtained by plotting log ([CuL$^\beta_2$]$_\infty$ − [CuL$^\beta_2$]$_t$) *vs.* time, which again gives a good pseudo-first-order plot at reaction times where the first step no longer interferes.

The $k_{obs.}$ value for the second step thus determined can be considered accurate, but $k_{obs.}$ for the first step is slightly altered because of the formation of [Cu(acac)$_2$] from [Cu(acac)L$^\beta$] (*via* ligand disproportionation), concomitant with the consumption of [Cu(acac)$_2$] due to C_2N_2 addition. An approximate estimate of this last effect indicates that the true cyanation rate of the first step may be 10% greater than the experimental one.

The observed $k_{obs.}$ values for both steps depend linearly upon C_2N_2 concentration as shown in Figure 6.

The resulting second-order rate constants are k_1 = 7.4 × 10^{-4} and k_2 = 1.7 × 10^{-4} dm^3 mol^{-1} s^{-1}, *i.e.* $k_1 \simeq 2\,k_2$ if statistical factors are considered. In other words, C_2N_2 exhibits the same reactivity towards [Cu(acac)$_2$] and [Cu(acac)L$^\beta$].

A final, remarkable result is the effect of the quality of the solvent on the reaction rate. Use of commercial CH_2Cl_2 (HCl 0.001%; H_2O 0.02%) leads to a four-fold increase in reactivity of C_2N_2 for both stages, with respect to the use of purified CH_2Cl_2.

The reported kinetic data for addition of C_2N_2 to [Cu(acac)$_2$] are consistent with the rate law (13). This means that

$$-\mathrm{d}[\mathrm{Cu(acac)_2}]/\mathrm{d}t = k_1[\mathrm{C_2N_2}][\mathrm{Cu(acac)_2}] \quad (13)$$

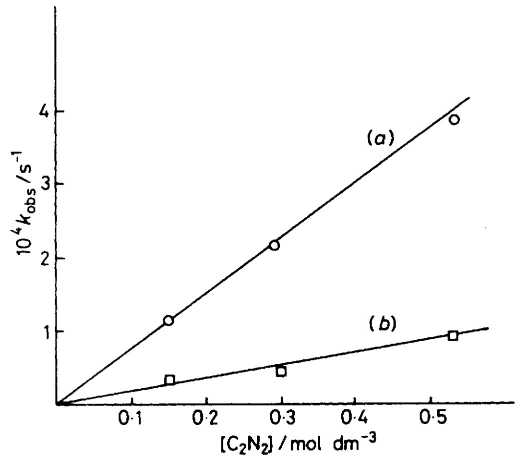

Figure 6. Dependence of $k_{obs.}$ on C_2N_2 concentration for (a) the first and (b) the second reaction step

C_2N_2 is co-ordinated to $[Cu(acac)_2]$ in the transition state. As to the details of the mechanism, this observation implies (i) C_2N_2 attack on the metal centre, (ii) transfer of C_2N_2 to the co-ordinated ligand, (iii) rearrangement of the resulting cyanoiminoacetylacetonate ligand from a type L^α to a type L^β structure. In principle, direct attack of C_2N_2 on the metal could give a five-co-ordinate reactive intermediate $[Cu(acac)_2(C_2N_2)]$,[14] which changes rapidly into the cyanoiminomethyl derivative upon insertion of cyanogen into the methine bond, but the effect of the acidity of the medium (and/or water content) strongly suggests that an alternative mechanism could operate. It is known that the ligand exchange reactions exhibited by some $[M(acac)_3]$ type complexes[15] involve preliminary acid- or water-assisted opening of a co-ordination arm, thus giving rise to a co-ordinatively 'unsaturated' metal complex. The remarkable kinetic effect due to HCl and H_2O in the solvent on the addition of C_2N_2 to $[Cu(acac)_2]$ strongly suggests that end-on co-ordination of C_2N_2 to a three-co-ordinate Cu^{II} centre, rather than to a four-co-ordinate $[Cu(acac)_2]$ moiety, may be the major process.

Indirect support for the importance of the fast preliminary ring-opening step is given by the observed fast exchange between $[Cu(acac)_2]$ and $[CuL^\beta{}_2]$ to give $[Cu(acac)L^\beta]$, and by the comparably fast substitution with protonation reaction between $[Cu(acac)_2]$ and HL^α in purified CH_2Cl_2. Since it is generally accepted[15] that these exchange reactions of β-diketonate complexes proceed through this ring-opening process, it seems reasonable that the 'slow' cyanogen addition to $[Cu(acac)_2]$ should imply this fast preliminary process.

Acknowledgements

We thank Mr. A. Ravazzolo for technical assistance.

References

1 (*a*) Part 2, B. Corain, C. Crotti, A. Del Pra, F. Filira, and G. Zanotti, *Inorg. Chem.*, 1981, **20**, 2044; (*b*) Part 1, B. Corain, A. Del Pra, F. Filira, and G. Zanotti, *ibid.*, 1979, **18**, 3523.
2 W. Traube, *Ber.*, 1898, **31**, 2938.
3 M. Basato, B. Corain, A. Marcomini, G. Valle, and G. Zanotti, *J. Organomet. Chem.*, submitted for publication.
4 B. Corain, M. Basato, and G. Bontempelli, *Anal. Chem.*, 1981, **53**, 124.
5 A. C. T. North, D. C. Phillips, and F. S. Mathews, *Acta Crystallogr., Sect. A*, 1968, **24**, 351.
6 R. Eisenberg and J. A. Ibers, *Inorg. Chem.*, 1965, **4**, 773.
7 'International Tables for *X*-Ray Crystallography,' Kynoch Press, Birmingham, 1974, vol. 4.
8 G. Sheldrick, SHELX 76 System of Computing Programs, University of Cambridge, 1976.
9 J. W. Carmichael, L. K. Steinauf, R. L. Belford, *J. Chem. Phys.*, 1965, **43**, 3959.
10 G. A. Barclay and A. Cooper, *J. Chem. Soc.*, 1965, 3746.
11 N. A. Bailey, D. E. Fenton, M. V. Franklin, and M. Hall, *J. Chem. Soc., Dalton Trans.*, 1980, 984; T. S. Moore and M. W. Young, *J. Chem. Soc.*, 1932, 2694; M. F. Farona, D. C. Perry, and H. A. Kuska, *Inorg. Chem.*, 1968, **7**, 2415; L. F. Nicholas and W. R. Walker, *Aust. J. Chem.*, 1970, **23**, 1135.
12 A. M. Fatta and R. L. Lintvedt, *Inorg. Chem.*, 1971, **10**, 478.
13 R. P. Eckberg, J. H. Nelson, J. W. Kenney, P. N. Howells, and R. A. Henry, *Inorg. Chem.*, 1977, **16**, 3128 and refs. therein.
14 D. P. Graddon, *Coord. Chem. Rev.*, 1969, **4**, 1.
15 A. Watanabe, H. Kido, and K. Saito, *Inorg. Chem.*, 1981, **20**, 1107, and refs. therein.

Received 17th *May* 1982; *Paper* 2/812